Development of a Low-Cost Lightweight Advanced K-band Horn Antenna with Charge-Programmed Deposition 3D Printing

Junbo Wang, Zhenpeng Xu, Zhen Wang, Xiaoyu Zheng, and Yahya Rahmat-Samii

Abstract—We present the first development of a lightweight, monolithic, circularly polarized (CP) K-band horn antenna developed using a novel charge-programmed deposition (CPD) manufacturing process. The horn has a polymer body with metalized interior surface. The CPD process creates complex geometries with programmed charged surfaces via three-dimensional (3D) printing and allows the deposition of metallics anywhere within the 3D layout. Intricate internal structures of the horn, such as the meandered waveguide transition and the septum polarizer, were successfully constructed. Measured patterns of the horn demonstrated great agreement with simulations, with an axial ratio below 2.5 dB in the range of 17.5 - 20.5 GHz. The total weight of the horn is only 11 g, marking a significant weight reduction of around 80% compared to traditionally fabricated horns of similar size and operating frequency. The low-cost and lightweight horn antennas enabled by this process can significantly benefit mass- and cost-sensitive applications such as small satellite and CubeSat missions.

Index Terms—Horn Antenna, Septum Polarizer, Circular Polarization, Lightweight Antenna, Additive Manufacturing, Charge-Programmed Deposition, 3D printing, Small Satellites, CubeSats, Space Antennas.

I. INTRODUCTION

HORN antennas are reliable, extensively studied, and widely applied in communications systems. Horn antennas can be designed to achieve competitive performance (polarization, bandwidth, cross-polarization suppression, etc.) through the incorporation of sophisticated features, such as spline profiles, corrugations, ridges, septums, etc. These complex geometrical features, while leveraging antenna performance, are very challenging to manufacture with traditional techniques such as computer numerical control (CNC) machining. The cost and accuracy of these traditional manufacturing methods get further challenged in higher frequencies such as millimeter-wave and beyond, where the geometrical features can be in the order of hundreds of microns or less. The advancement in additive manufacturing (AM) techniques have offered new low-cost approaches for the manufacturing of advanced horn antennas with exotic geometrical features [1].

The AM techniques demonstrated for antenna manufacturing can be divided into two major categories, depending on

Manuscript created January, 2023; J. Wang and Y. Rahmat-Samii are with the Department of Electrical and Computer Engineering at University of California, Los Angeles, CA 90095, USA. Z. Xu, Z. Wang, and X. Zheng are with the Department of Civil and Environmental Engineering at University of California, Los Angeles, CA 90095, USA. and the Department of Materials Science and Engineering at University of California, Berkeley, CA 94720, USA. (Email: wangjunbo@ucla.edu, xuzhenpeng@ucla.edu, zwang19@ucla.edu, rayne@seas.ucla.edu, rahmat@ee.ucla.edu)
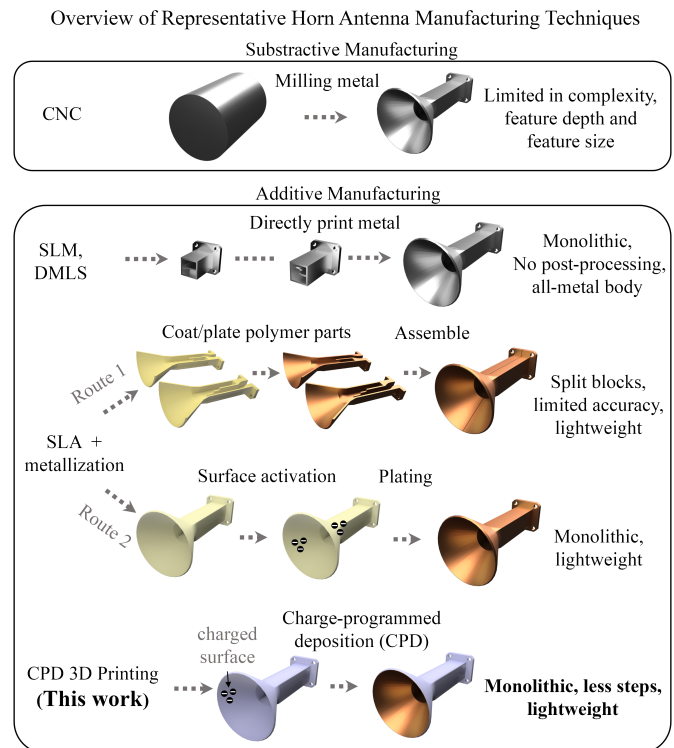

Fig. 1. Overview of the representative horn manufacturing techniques and a comparison of their key characteristics.

whether metal is the only material involved. Selective Laser Melting (SLM) and Direct Metal Laser Sintering (DMLS) are the metal-printing AM methods that have been used for fabricating horn antennas [2]–[5]. The advantage of this category is that the horn with complex geometries can be monolithically printed in metal and does not require additional processing. These methods yield good printing accuracy (tens of microns) and have been used for horn antennas from microwave up to terahertz ranges [2]–[5].

The other category of techniques fabricate the horn by first 3D-printing the body using polymer and then performing surface metallization [6]–[12]. This leads to significantly lighter antennas compared to their traditional all-metal versions. Therefore, these techniques show promise for emerging small satellite and CubeSat applications where the weight of the antenna becomes critical [9], [13]. Typically, these processes utilize Fused Deposition Modeling (FDM) or Stereolithography (SLA) to first construct a lightweight polymer body of the

horn, and then perform plating to establish the conductive surface of the horn. Several plating methods have been reported in the literature. One of the methods is to apply conductive spray to the surface of the SLA-printed components [9], but it requires a "split-block" design so that the internal structures of the horn/waveguide can be exposed for thorough coating. This method raises the concern for tolerances because of the assembling process involved. Electroless plating is another technique that has become popular for the metallization of complex devices as it makes it possible to perform plating in monolithic structures with complex internal features (Fig. 1). Electroless plating requires chemical treatment to first activate the surface of the SLA-printed component before it can be submerged in the coating solution for metal deposition. The conductive coating should have a thickness of at least three skin depths [10], [11] to avoid RF leakage. Electroplating can be used to improve the plating thickness once a surface metallization is formed. Waveguides and horns fabricated by such "polymer + metallization" processes have also been demonstrated from tens to hundreds of GHz [9]–[12].

Charge-programmed deposition (CPD) process recently emerged as an intriguing AM technique for manufacturing complex electronic devices [14]. Compared with other existing AM techniques, the key advantage of the CPD process is being able to build interpenetrated dielectric and metallic material in a unified process. the CPD process contains two major steps: 1) micro-SLA that develops the polymer structure with a programmable charged surface area; 2) selective metal deposition that forms metallization on the charged surface area (Fig. 1). The micro-SLA process yield a resolution of 50 μm in xy direction and $25 - 100$ μm in z direction [15]. The metallization thickness is typically in the order of hundreds of nanometers to several micrometers. This method demonstrates appealing advantages in terms of advanced horn antenna fabrications because the charged surface is already monolithically built into the polymer body of the horn and surface activation is no longer required. The time and procedures involved in the antenna fabrication are thus considerably reduced. Such a one-step process with customizable free-form factors and individually addressable 3D interfaces is not achievable in other approaches.

In this work, we for the first time introduce the CPD process to the monolithic fabrication of advanced horn antennas. In particular, we demonstrate the development of a lightweight, circularly polarized (CP) K-band horn antenna. The horn has intricate internal features including a stepped septum polarizer, a meandered waveguide transition, and a square-to-circular waveguide adapter.

II. DESIGN OF THE CIRCULARLY-POLARIZED HORN WITH SEPTUM POLARIZER

The horn in this work is designed for K-band at the center frequency of 19 GHz. Although the horn will be built in one piece with a monolithic body, the three segments of the horn considering their functionality are presented as separated parts in Fig. 2 for illustrative purposes. The three segments are: (1) the circular horn with a rectangular-to-circular waveguide
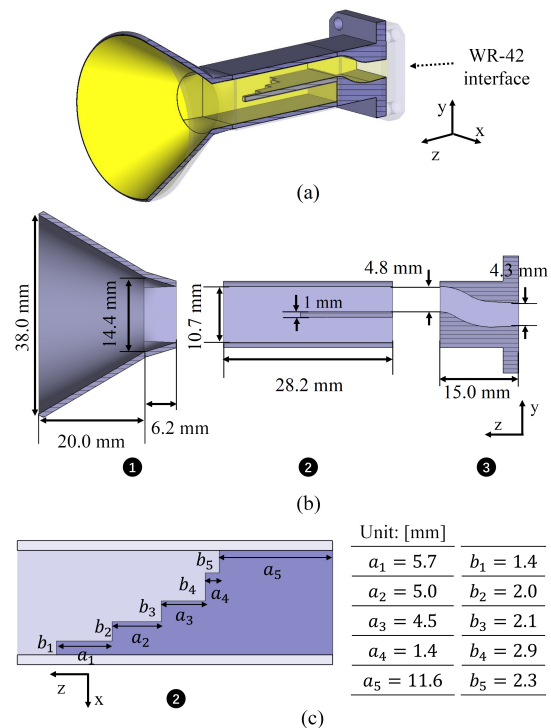

Fig. 2. The CP septum horn designed to be manufactured using the CPD process. (a) Overview of the designed horn that has a monolithic polymer body and copper coating on the interior surface. (b) The cross-section of the horn in the $y - z$ plane. The three segments are separated for a better illustration of the design. (c) The septum polarizer section shown in the $x - z$ plane and the parameters of the stepped septum.

Unit: [mm]	
$a_1 = 5.7$	$b_1 = 1.4$
$a_2 = 5.0$	$b_2 = 2.0$
$a_3 = 4.5$	$b_3 = 2.1$
$a_4 = 1.4$	$b_4 = 2.9$
$a_5 = 11.6$	$b_5 = 2.3$

adapter; (2) the polarizer consisting of a square waveguide and a stepped septum; (3) the meandered waveguide transition from a WR-42 interface to one port of the polarizer. The horn is designed to be compatible with a commercially available coax-to-WR-42 adapter that will be used for excitation. The detailed designed parameters are shown in Fig. 2.

The septum polarizer (segment 2) is the key section for the wideband CP performance of the horn. Septum polarizer is a widely applied structure in waveguide devices and horn antennas to generate high-purity circular polarization in a wide bandwidth [16]. The stepped septum is the most common configuration, while smooth septums with optimized profiles have also been proposed to improve the power handling capability [17]. In this work, a 5-stage stepped septum is employed and the dimensions of the stages are optimized (with particle swarm optimization [18]) based on the initial geometry suggested in [16] [Fig. 2(c)]. The width of the square waveguide is chosen to match the longer dimension of the WR-42 waveguide to minimize mismatch.

The typical working condition of a septum polarizer is to excite one port of the septum polarizer with the other port terminated with a matched load [3], [19]. While this allows the horn to radiate dual CP, it also increases the profile and weight of the horn, which may not be favorable in certain scenarios. When a septum polarizer is optimized, the two ports usually have good isolation such that terminating one port of the polarizer with a closed cavity does not impact the performance of the polarizer [2], [20]. Adopting such a design allows the
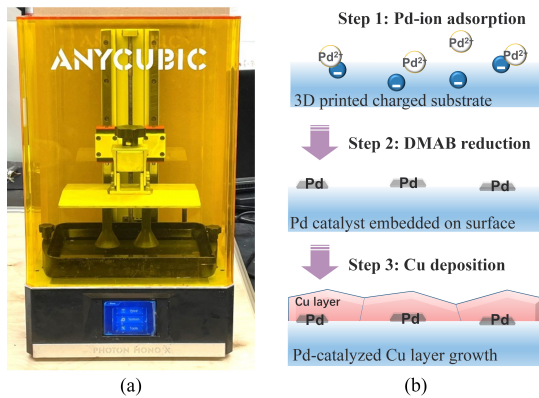
Fig. 3. (a) The polymer body of the horn being printed in the printer. (b) The schematic illustration of the Cu-deposition procedure.

horn to have a single excitation port and makes the horn more compact. However, this also makes the feeding port to be offset from the center axis of the horn (as in [2], [20]). To make the horn easier to align, we introduce the meandered waveguide transition (segment 3) to align the center of the waveguide port onto the center axis of the horn. Segment 3 also provides a smooth transition that matches the polarizer port with the WR-42 interface that has slightly different dimensions.

It is also worth noting that the three segments can potentially be manufactured as modularized parts to enable a polarization reconfigurable design: by simply changing the orientation of segment 3, one can switch the polarizer port being excited and realize either right-hand CP (RHCP) or left-hand CP (LHCP) radiation. For the monolithic horn demonstrated in this paper, the excited port is chosen such that RHCP radiation is generated.

III. FABRICATION OF THE HORN WITH CHARGE-PROGRAMMED DEPOSITION 3D PRINTING

The body of the horn was 3D printed by a commercial printer, Anycubic Photon Mono X (Anycubic Inc.) [15]. The printer was equipped with a high-resolution LCD screen to selectively cure the resin with predefined areas and build the 3D structures layer by layer [Fig. 3(a)]. The resin was composed of a commercial rigid resin (Formlabs tough 2k, Formlabs Inc.) and bis(2-(methacrylooyloxy)ethyl))phosphate (PDD, Sigma-Aldrich Inc.) in a 90:10 mass ratio. The commercial rigid resin served as the matrix for the structure. PDD provided the negatively charged site to immobilize the Pd ion for catalyzing the following metal deposition.

After the body of the horn was printed, an aqueous solution of tetraamminepalladium(II) chloride monohydrate (Sigma-Aldrich Inc.) of 1.4 mg/mL was added fully into the inner chamber of the horn. In 2-5 minutes, the Pd ions were anchored by PDD to the interior surface of the horn's chamber. After rinsing the horn with deionized water and drying with compressed air, an aqueous solution of borane dimethylamine complex (DMAB, Sigma-Aldrich Inc.) of 0.7 mg/mL was filled into the chamber and kept for 5 min to reduce the immobilized Pd ions into Pd nanoparticles with catalytic activity. Finally, a Cu electroless plating solution (1:1 mixture of parts A and B of the electroless Cu kit from Caswell Inc.) filled up the horn and plated Cu under the catalysis by Pd.
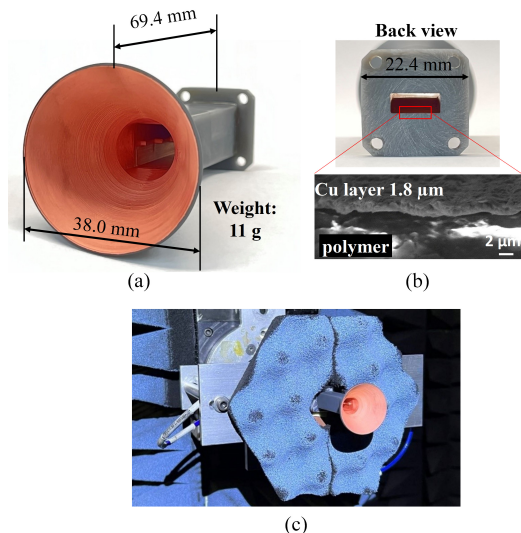

Fig. 4. Photos of the fabricated horn and antenna measurement setup. (a) The completed horn after copper deposition. (b) The rectangular waveguide interface of the horn and the scanning electron microscope (SEM) image showing the plating thickness. (c) The horn being measured for its radiation pattern in the spherical near-field range at UCLA.
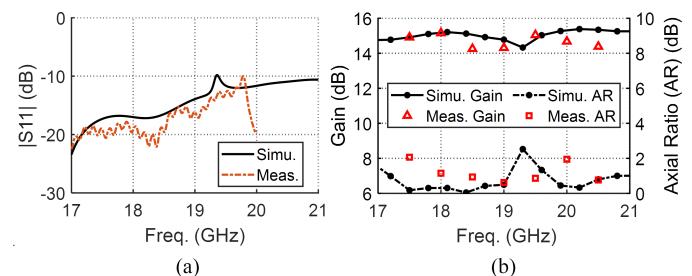

Fig. 5. (a) Simulated and measured reflection coefficient $|S_{11}|$ of the horn when excited using a coax-to-WR-42 waveguide adapter. (b) Simulated versus measured gain and axial ratio (AR) of the horn.

This process lasted 3 hours to meet the metallization thickness requirement (greater than three skin depths, skin depth at 19 GHz is 0.473 μm). This procedure of copper deposition is illustrated in Fig. 3(b).

After rinsing, drying, and polishing the bottom, the horn was obtained as shown in Fig. 4. The entire manufacturing process, including printing, plating, and post-processing, can be completed in a day at a low material cost. The weight of the horn is only 11 g, which marks around 80% of weight reduction compared to a traditionally manufactured all-metal horn of similar size at this frequency (referring to standard gain horn Narda 638). The copper coating has a thickness around 1.8 μm (more than three times skin depth for this frequency range) according to the scanning electron microscope (SEM) image of a representative sample of the horn [Fig. 4 (b)].

IV. MEASUREMENT RESULTS OF THE HORN ANTENNA

The fabricated horn was assembled with a coax-to-WR-42 waveguide adapter from Narda. To be consistent with the measurement setup, in simulations, the CAD model of a representative adapter was assembled with the horn. The horn was then excited from the 50-ohm coax port of the adapter. While the WR-42 waveguide is rated for 18.0 - 26.5 GHz, its cut-off frequency is about 14.1 GHz and thus we performed
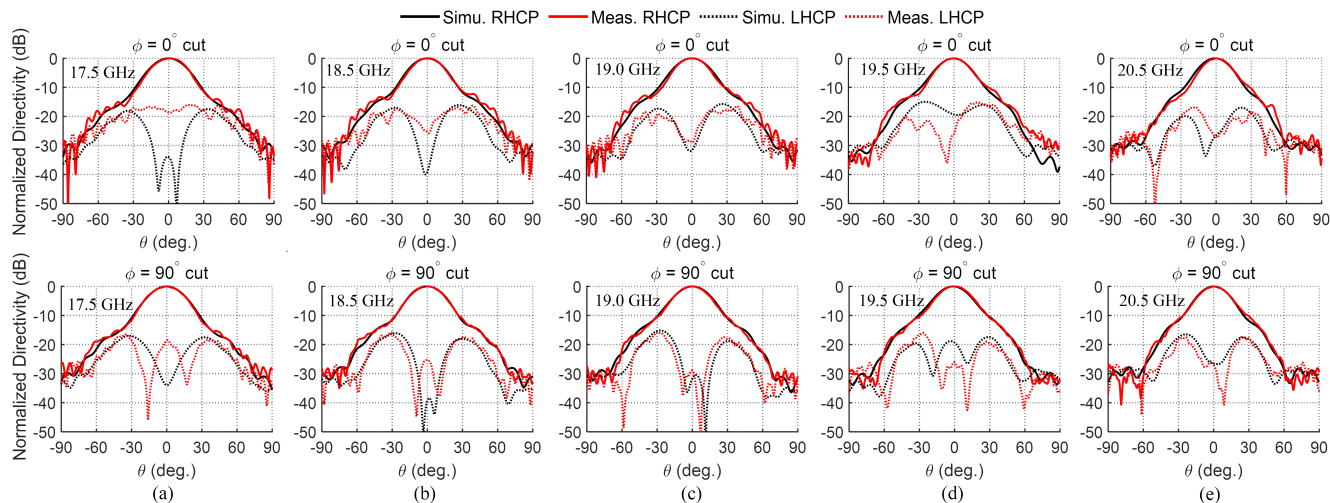
Fig. 6. (a)-(e) Measured versus simulated RCHP and LHCP radiation patterns of the horn in two orthogonal cuts, at representative frequencies from 17.5 to 20.5 GHz. The measured RHCP directivity for the presented frequencies are 15.05 dBi, 15.26 dBi, 15.29 dBi, 15.37 dBi, and 15.97 dBi, respectively.

the simulation in the frequency range of 17.0 to 21.0 GHz. The simulated and measured reflection coefficients (S_{11}) are shown in Fig. 5(a). Limited by the frequency range of the vector network analyzer, the S_{11} was only measured up to 20.0 GHz. Nonetheless, the measured S_{11} is below -10 dB in the frequency range considered and agrees well with the simulated result. The minor differences can be attributed to fabrication tolerances, measurement uncertainties, and slight variations between the simulated adapter and the actual part used. In simulations there appeared to be a resonance near 19.36 GHz, causing a hump in the S_{11} and a slight degradation in axial ratio (AR) and directivity [Fig. 5(b)]. This is related to a resonance in the septum polarizer section and it is caused by the reflection at the circular-to-square adapter (segment 1). While using a longer circular-to-square transition section can help reduce the reflection, it will also increase the total length of the horn. The current horn design still well satisfies our objective to demonstrate the CPD process's capability in manufacturing complex horn antennas.

The radiation pattern of the horn was then measured in the spherical near-field range at UCLA [Fig. 4(c)]. The measured CP patterns in the two orthogonal cuts of the horn are presented in Fig. 6 for representative frequencies from 17.5 to 20.5 GHz. Excellent agreement with the simulated patterns can be observed for most of the frequency samples, justifying that all the features of the horn were manufactured with good accuracy. The measured RHCP directivity for 17.5, 19.0, and 20.5 GHz are 15.05 dBi, 15.29 dBi, and 15.97 dBi, respectively. The measured broadside AR across the frequency band is well below 2.5 dB [Fig. 5(b)]. The slight differences compared to the simulations can be due to the fabrication tolerances and measurement uncertainties that can not be fully represented in simulations.

The gain of the fabricated horn is measured via the substitution method by referencing a Narda 638 standard gain horn. Overall, the measured gain appeared to be slightly lower than the simulated gain [Fig. 5(b)]. This can be attributed to the fact that the simulation model assumed an ideal copper coating with a smooth surface, whereas in reality, the layering effect

of SLA can increase the surface roughness of the coated metal, leading to increased ohmic loss [12]. At the center frequency 19 GHz, the measured gain is 14.31 dB, corresponding to a measured gain loss of 0.98 dB. The measured return loss based on the measured S_{11} (-16 dB) is around 0.11 dB, and the residual of the loss (0.87 dB) is attributed mainly to the ohmic loss in the copper coating. This value is also comparable to the loss that has been reported in the literature for horn antennas built using other "SLA + metallization" processes [10]–[12]. However, it is anticipated that improvement in the ohmic loss can be achieved by improved metal deposition, e.g., through additional electroplating processes.

V. CONCLUSIONS

The charge-programmed deposition (CPD) 3D printing method is a novel additive manufacturing technology that can unlock new possibilities for designing and manufacturing advanced horn antennas. The ability to program charged surfaces in complex monolithic geometry significantly simplifies the metallization process compared to other horn antenna manufacturing techniques. In this work, a K-band CP septum horn was designed and manufactured using the CPD process. The horn is a monolithic design consisting of a meandered waveguide transition, a stepped-septum polarizer, and a circular horn adapted to a square waveguide. The horn has a polymer body and copper-plated interior surface. The measured results of reflection coefficient and radiation patterns in 17.5-20.5 GHz indicate the promising quality of the manufactured horn. The printed horn weighs only 11 g thanks to the lightweight polymer body used. The lightweight and low-cost horn antenna with a monolithic body can largely benefit applications with critical requirements on mass, e.g., for small satellites and CubeSats. While demonstrated at 19 GHz, it is anticipated that this technology can be applicable for horn antennas in the millimeter-wave range as well. This demonstration marks the first successful development of an advanced horn antenna using the novel CPD process and opens up appealing design and fabrication possibilities for horn antennas and other advanced waveguide devices.

REFERENCES

[1] D. Helena, A. Ramos, T. Varum, and J. N. Matos, "Antenna design using modern additive manufacturing technology: A review," *IEEE Access*, vol. 8, pp. 177064–177083, 2020.

[2] K. Kotzé and J. Gilmore, "Slm 3d-printed horn antenna for satellite communications at x-band," in *2019 IEEE-APS Topical Conference on Antennas and Propagation in Wireless Communications (APWC)*, pp. 148–153, 2019.

[3] M. J. Veljovic and A. K. Skrivervik, "Circularly polarized axially corrugated feed horn for cubesat reflectarray applications," in *2020 14th European Conference on Antennas and Propagation (EuCAP)*, pp. 1–4, 2020.

[4] N. Luo, G. Mishra, S. K. Sharma, and X. Yu, "Experimental verification of 3d metal printed dual circular-polarized horn antenna at v-band," in *2019 Antenna Measurement Techniques Association Symposium (AMTA)*, pp. 1–6, 2019.

[5] A. Reinhardt, M. Möbius-Labinski, C. Asmus, A. Bauereiss, and M. Höft, "Additive manufacturing of 300 ghz corrugated horn antennas," in *2019 IEEE MTT-S International Microwave Workshop Series on Advanced Materials and Processes for RF and THz Applications (IMWS-AMP)*, pp. 40–42, 2019.

[6] E. G. Geterud, P. Bergmark, and J. Yang, "Lightweight waveguide and antenna components using plating on plastics," in *2013 7th European Conference on Antennas and Propagation (EuCAP)*, pp. 1812–1815, 2013.

[7] P. T. Timbie, J. Grade, D. van der Weide, B. Maffei, and G. Pisano, "Stereolithographed mm-wave corrugated horn antennas," in *2011 International Conference on Infrared, Millimeter, and Terahertz Waves*, pp. 1–3, 2011.

[8] J.-C. S. Chieh, B. Dick, S. Loui, and J. D. Rockway, "Development of a ku-band corrugated conical horn using 3-d print technology," *IEEE Antennas and Wireless Propag. Lett.*, vol. 13, pp. 201–204, 2014.

[9] J. S. Silva, M. García-Vigueras, T. Debogović, J. R. Costa, C. A. Fernandes, and J. R. Mosig, "Stereolithography-based antennas for satellite communications in ka-band," *Proc. of the IEEE*, vol. 105, no. 4, pp. 655–667, 2017.

[10] A. Macor, E. De Rijk, S. Alberti, T. Goodman, and J.-P. Ansermet, "Note: Three-dimensional stereolithography for millimeter wave and terahertz applications," *Rev. Sci. Instrum.*, vol. 83, no. 4, p. 046103, 2012.

[11] A. I. Dimitriadis, T. Debogović, M. Favre, M. Billod, L. Barloggio, J.-P. Ansermet, and E. De Rijk, "Polymer-based additive manufacturing of high-performance waveguide and antenna components," *Proc. of the IEEE*, vol. 105, no. 4, pp. 668–676, 2017.

[12] J. Teniente, J. C. Iriarte, R. Caballero, D. Valcázar, M. Goñi, and A. Martínez, "3-d printed horn antennas and components performance for space and telecommunications," *IEEE Antennas and Wireless Propag. Lett.*, vol. 17, no. 11, pp. 2070–2074, 2018.

[13] Y. Rahmat-Samii, V. Manohar, and J. M. Kovitz, "For satellites, think small, dream big: A review of recent antenna developments for cubesats.," *IEEE Antennas and Propag. Mag.*, vol. 59, no. 2, pp. 22–30, 2017.

[14] R. Hensleigh, H. Cui, Z. Xu, J. Massman, D. Yao, J. Berrigan, and X. Zheng, "Charge-programmed three-dimensional printing for multi-material electronic devices," *Nat. Electron.*, vol. 3, pp. 1–9, 04 2020.

[15] "Anycubic 3d printing", https://www.anycubic.com/products/anycubic-photon-s, (accessed Nov. 20, 2022)

[16] M. Chen and G. Tsandoulas, "A wide-band square-waveguide array polarizer," *IEEE Trans. on Antennas and Propag.*, vol. 21, no. 3, pp. 389–391, 1973.

[17] I. Kim, J. M. Kovitz, and Y. Rahmat-Samii, "Enhancing the power capabilities of the stepped septum using an optimized smooth sigmoid profile," *IEEE Antennas and Propag. Mag.*, vol. 56, no. 5, pp. 16–42, 2014.

[18] J. Robinson and Y. Rahmat-Samii, "Particle swarm optimization in electromagnetics," *IEEE Trans. on Antennas and Propag.*, vol. 52, no. 2, pp. 397–407, 2004.

[19] C. Shu, J. Wang, S. Hu, Y. Yao, J. Yu, Y. Alfadhl, and X. Chen, "A wideband dual-circular-polarization horn antenna for mmwave wireless communications," *IEEE Antennas and Wireless Propag. Lett.*, vol. 18, no. 9, pp. 1726–1730, 2019.

[20] Y. Huang, J. Geng, R. Jin, X. Liang, X. Bai, X. Zhu, and C. Zhang, "A novel compact circularly polarized horn antenna," in *2014 IEEE Antennas and Propagation Society International Symposium (APSURSI)*, pp. 43–44, 2014.